Electronic Supplementary Material (ESI) for Inorganic Chemistry Frontiers.

Supporting Information

Reversible step spin crossover modulation via water absorption and dehydration in a 3D Hofmann-type framework

Kai-Ting Lian, Wei-Wei Wu, Guo-Zhang Huang, Yang Liu, Si-Guo Wu,

Zhao-Ping Ni* and Ming-Liang Tong

Key Laboratory of Bioinorganic and Synthetic Chemistry of Ministry of Education,

School of Chemistry, Sun Yat-Sen University, Guangzhou, 510275, P. R. China

Contents

Table S1. Crystallographic data for **1·dpt·2.5H$_2$O**.

Parameter	**1·dpt·2.5H$_2$O**		
T /K	80(2)	150(2)	298(2)
Chemical Formula	$C_{64}H_{41}Fe_2N_{16}O_{0.5}Pt_2S_4$	$C_{64}H_{41}Fe_2N_{16}O_{0.5}Pt_2S_4$	$C_{64}H_{41}Fe_2N_{16}O_{0.5}Pt_2S_4$
Mr	1672.25	1672.25	1672.25
Crystal system	monoclinic	monoclinic	monoclinic
Space group	$P2_1/C$	$P2_1/C$	$P2_1/C$
a/Å	7.1865(2)	7.2691(3)	7.4493(3)
b/Å	28.8122(8)	28.9451(10)	29.2894(10)
c/Å	29.7515(9)	29.9141(12)	30.2310(11)
α/°	90	90	90
β/°	94.6390(10)	94.9550(10)	94.5640(10)
γ/°	90	90	90
V/Å^3	6140.1(3)	6270.5(4)	6575.1(4)
Z	4	4	4
μ(Mo Kα)/mm^{-1}	5.199	5.090	4.855
Radiation	Mo Kα (λ = 0.71073)	Mo Kα (λ = 0.71073)	Mo Kα (λ = 0.71073)
Reflections collected	65816	128886	57550
Independent reflections	14067 [R_{int} = 0.0514]	14424 [R_{int} = 0.0578]	15070 [R_{int} = 0.0279]
Goodness-of-fit on F^2	1.256	1.135	1.076
Final R indexes [I>=2σ (I)]	R_1[a] = 0.0747, wR_2 = 0.1452	R_1 = 0.0469, wR_2 = 0.0985	R_1 = 0.0306, wR_2 = 0.0634
Final R indexes [all data]	R_1 = 0.0885, wR_2[b] = 0.1497	R_1 = 0.0548, wR_2 = 0.1010	R_1 = 0.0424, wR_2 = 0.0668
Largest diff. peak/hole / e Å^{-3}	2.70/-3.18	2.66/-2.17	1.86/-1.39
CCDC	2088653	2088655	2088654

[a] $R_1 = \Sigma||F_o| - |F_c||/\Sigma|F_o|$; [b] $wR_2 = \{[\Sigma w(F_o^2-F_c^2)^2]/\Sigma[w(F_o^2)^2]\}^{1/2}$.

Table S2. Crystallographic data for **1·dpt·1.5H$_2$O**.

Parameter	**1·dpt·1.5H$_2$O**		
T /K	80(2)	180(2)	298(2)
Chemical Formula	$C_{64}H_{41}Fe_2N_{16}O_{0.5}Pt_2S_4$	$C_{64}H_{41}Fe_2N_{16}O_{0.5}Pt_2S_4$	$C_{64}H_{41}Fe_2N_{16}O_{0.5}Pt_2S_4$
*M*r	1672.25	1672.25	1672.25
Crystal system	monoclinic	monoclinic	monoclinic
Space group	$P2_1/C$	$P2_1/C$	$P2_1/C$
a/Å	7.1406(3)	7.2864(4)	7.4466(7)
b/Å	28.6586(10)	28.9521(15)	29.242(3)
c/Å	29.6734(11)	29.9614(15)	30.236(3)
α/°	90	90	90
β/°	94.8413(13)	95.435(2)	95.000(3)
γ/°	90	90	90
V/Å^3	6050.7(4)	6292.1(6)	6559.1(10)
Z	4	4	4
μ(Mo Kα)/mm^{-1}	5.275	5.073	4.867
Radiation	Mo Kα (λ = 0.71073)	Mo Kα (λ = 0.71073)	Mo Kα (λ = 0.71073)
Reflections collected	45352	116856	114467
Independent reflections	12339 [R_{int} = 0.0592]	12831 [R_{int} = 0.0654]	13384 [R_{int} = 0.0776]
Goodness-of-fit on F^2	1.076	1.115	1.237
Final *R* indexes [*I*>=2σ (*I*)]	R_1[a] = 0.0409, wR_2 = 0.0953	R_1 = 0.0411, wR_2 = 0.0900	R_1 = 0.0582, wR_2 = 0.1101
Final *R* indexes [all data]	R_1 = 0.0634, wR_2[b] = 0.1030	R_1 = 0.0519, wR_2 = 0.0941	R_1 = 0.0721, wR_2 = 0.1140
Largest diff. peak/hole / e Å^{-3}	2.20/-1.24	2.04/-1.67	1.73/-2.60
CCDC	2088656	2088657	2088658

[a] $R_1 = \Sigma||F_o| - |F_c||/\Sigma|F_o|$; [b] $wR_2 = \{[\Sigma w(F_o^2-F_c^2)^2]/\Sigma[w(F_o^2)^2]\}^{1/2}$.

Table S3. Selected structural parameters for **1·dpt·2.5H$_2$O** at different temperatures.

Parameter	80(2)	150(2)	298(2)
<Fe-N>[a]	<Fe1-N> 1.966(9) <Fe2-N> 2.053(9)	<Fe1-N> 1.961(5) <Fe2-N> 2.167(5)	<Fe1-N> 2.171(3) <Fe2-N> 2.172(3)
Fe···Fe[b]	14.9491(20) 14.8031(20)	15.0284(14) 14.8885(14)	15.1875(10) 15.0451(10)
Fe···Fe[c]	10.1414(19) 10.2136(19) 10.1673(19) 10.2518(19)	10.2386(12) 10.3240(12) 10.2298(12) 10.3387(12)	10.5071(8) 10.4318(8) 10.4322(8) 10.5166(8)
ΣFe[d]	ΣFe1 11.4(3) ΣFe2 17.8(3)	ΣFe1 11.7(2) ΣFe2 26.8(2)	ΣFe1 15.49(14) ΣFe2 19.16(14)
Fe-N≡C[e]	Fe1-N≡C 175.6(8) Fe2-N≡C 169.5(8)	Fe1-N≡C 175.6(5) Fe2-N≡C 166.8(5)	Fe1-N≡C 172.9(4) Fe2-N≡C 166.5(4)
θ[f]	89.593(22) 89.526(22)	89.393(13) 89.524(13)	89.539(9) 89.587(9)
dihedral angle[g]	Fe1S1:9.378(388)/10.410(728); 10.854(323) Fe2S2:6.701(384)/7.311(385); 3.414(284)	Fe1S1:9.919(302)/8.947(683); 11.262(256) Fe2S2:5.316(218)/6.913(269); 4.233(199)	Fe1S1:7.235(525)/9.907(593); 10.556(171) Fe2S2:3.731(208)/6.865(216); 3.988(172)
dihedral angle[h]	Fe1:10.210(307) Fe2:13.579(394)	Fe1:9.372(235) Fe2:15.375(262)	Fe1:12.868(179) Fe2:14.348(212)
dihedral angle[i]	S4:17.438(518)/17.742(749); 11.352(349) S3:16.650(755)/23.605(552); 13.129(391)	S4:17.692(410)/17.272(465); 10.753(260) S3:16.062(664)/21.810(451); 12.789(326)	S4:16.177(256)/17.926(463); 11.750(266) S3:15.639(661)/22.752(497); 13.407(232)
θ(N5-dpt1^{center}-N6)[j]	155.827(110)	155.451(76)	154.402(48)
θ(N11-dpt2^{center}-N12)[k]	153.384(130)	152.375(78)	151.527(51)

[a] The average Fe-N bond lengths(Å); [b] The Fe···Fe distance(Å) linked by dpt; [c] The Fe···Fe distance(Å) linked by $[Pt(CN)_4]^{2-}$; [d] Octahedral distortion parameters (°); [e] Average Fe-N≡C angles within Hofmann layer; [f] The acute angle between neighboring Fe(Ⅱ) sites within the Hofmann layer; [g] In the ligand dpt, the dihedral angles between thiadiazole and each pyridine ring as well as the dihedral angle between the pyridine rings; [h] The dihedral angle between the up and down pyridine rings coordinated to Fe(Ⅱ) site. [i] The dihedral angel between the pyridine rings in the unoccupied ligand dpt. [j] The angle for N5-dpt1^{center}-N6. [k] The angle for N11-dpt2^{center}-N12.

Table S4. Selected structural parameters for **1·dpt·1.5H$_2$O** at different temperatures.

Parameter	80(2)	180(2)	298(2)
<Fe-N>[a]	<Fe1-N> 1.964(5) <Fe2-N> 1.964(5)	<Fe1-N> 1.962(5) <Fe2-N> 2.169(5)	<Fe1-N> 2.167(7) <Fe2-N> 2.170(8)
Fe···Fe[b]	14.8787(14) 14.7948(14)	15.0440(15) 14.9190(15)	15.1912(23) 15.0472(23)
Fe···Fe[c]	10.1030(12) 10.1487(12) 10.0903(13) 10.1731(12)	10.2579(12) 10.3401(12) 10.2321(12) 10.3458(12)	10.4238(18) 10.5164(18) 10.5072(18) 10.4111(18)
*Σ*Fe[d]	ΣFe1 9.8 (2) ΣFe2 14.4(2)	ΣFe1 10.8(2) ΣFe2 23.19(2)	ΣFe1 15.4 (3) ΣFe2 19.2(3)
Fe-N≡C[e]	Fe1-N≡C 175.8(5) Fe2-N≡C 172.0(5)	Fe1-N≡C 175.7(5) Fe2-N≡C 167.2(5)	Fe1-N≡C 172.6(8) Fe2-N≡C 166.1(8)
θ[f]	89.532(14) 89.741(14)	89.367(13) 89.543(13)	89.473(18) 89.493(18)
dihedral angle[g]	Fe1S1:9.384(329)/11.456(324); 10.842(215) Fe2S2:7.131(236)/8.138(243); 2.427(207)	Fe1S1:10.147(285)/9.281(536); 11.542(227) Fe2S2:5.772(202)/6.429(240); 3.473(204)	Fe1S1:7.009(601)/9.939(656); 10.612(313) Fe2S2:4.718(360)/7.286(635); 4.024(340)
dihedral angle[h]	Fe1:9.933(234) Fe2:11.857(240)	Fe1:9.219(218) Fe2:14.940(268)	Fe1:12.959(358) Fe2:14.256(386)
dihedral angle[i]	S4:18.161(244)/18.767(284); 13.481(245) S3:16.471(758)/23.044(517); 14.549(256)	S4:18.058(304)/17.363(382); 11.014(274) S3:16.604(793)/22.224(536); 14.048(293)	S4:17.576(416)/18.405(588); 12.308(416) S3:15.612(524)/22.373(491); 13.389(417)
θ(N5-dpt1^{center}-N6)[j]	156.399(71)	155.590(76)	154.653(88)
θ(N11-dpt2^{center}-N12)[k]	154.670(71)	153.094(78)	152.275(132)

[a] The average Fe-N bond lengths(Å); [b] The Fe···Fe distance(Å) linked by dpt; [c] The Fe···Fe distance(Å) linked by $[Pt(CN)_4]^{2-}$; [d] Octahedral distortion parameters (°); [e] Average Fe-N≡C angles within Hofmann layer; [f] The acute angle between neighboring Fe(Ⅱ) sites within the Hofmann layer; [g] In the ligand dpt, the dihedral angles between thiadiazole and each pyridine ring as well as the dihedral angle between the pyridine rings; [h] The dihedral angle between the up and down pyridine rings coordinated to Fe(Ⅱ) site. [i] The dihedral angels between thiadiazole and each pyridine ring as well as the dihedral angle between the pyridine rings in the unoccupied ligand dpt. [j] The angle for N5-dpt1^{center}-N6. [k] The angle for N11-dpt2^{center}-N12.

Table S5. π···π interactions in **1·dpt·2.5H$_2$O** at different temperatures.

80 K	θ[1]	Z[2]	d[3]	r[4]
py1[a] and py2[b]	11.411(397)	3.7334(1)	3.5973	0.9989
py2[b] and py3[c]	11.411(397)	3.6324(1)	3.3323	1.4457
py5[e] and py6[f]	5.289(370)	3.4533(1)	3.3798	0.5022
py7[g] and py8[h]	5.681(357)	3.7216(1)	3.6477	0.7380
py8[h] and py9[i]	5.681(357)	3.7118(1)	3.3914	1.5086
py11[k] and py12[l]	6.317(330)	3.7206(1)	3.6574	0.6828
150 K	θ[1]	Z[2]	d[3]	r[4]
py1[a] and py2[b]	12.06(52)	3.7501(2)	3.6334	0.9282
py2[b] and py3[c]	12.060(396)	3.6872(1)	3.3621	1.5138
py5[e] and py6[f]	6.017(303)	3.4956(1)	3.4319	0.6642
py7[g] and py8[h]	4.873(641)	3.7686(1)	3.6871	0.7795
py8[h] and py9[i]	4.872(414)	3.7330(1)	3.4386	1.4530
py11[k] and py12[l]	6.828(261)	3.7656(1)	3.7018	0.6902
298 K	θ[1]	Z[2]	d[3]	r[4]
py1[a] and py2[b]	10.464(184)	3.7826(2)	3.6738	0.9007
py2[b] and py3[c]	10.464(184)	3.7508(1)	3.5315	1.2637
py5[e] and py6[f]	6.510(214)	3.6163(1)	3.5564	0.6555
py7[g] and py8[h]	4.236(224)	3.8469(1)	3.7562	0.8304
py8[h] and py9[i]	4.236(224)	3.8638(1)	3.5605	1.5006
py11[k] and py12[l]	5.814(250)	3.8144(1)	3.7683	0.5912

[a]py1: C5-C9, N5, x, y, z; [b]py2: C60-C64, N16, 1-x, 1/2+y, 1/2-z; [c]py3: C5'-C9', N5', 1+x, y, z; [e]py5: C37-C41, N13, x, 3/2-y, 1/2+z; [f]py6: C14'-C18', N6', 1+x, y, z; [g]py7: C32-C36, N12, x, 3/2-y, 1/2+z; [h]py8: C51-C55, N15, 1-x, 1/2+y, 1/2-z; [i]py9: C32'-C36', N12', 1+x, 3/2-y, 1/2+z; [k]py11: C46-C50, N14, x, 3/2-y, 1/2+z; [l]py12: C23'-C27', N11', 1+x, 3/2-y, 1/2+z.

[1] The dihedral angle between two aromatic rings (°); [2] The distance between the centroids of aromatic rings (Å); [3] The perpendicular distance between two aromatic rings (Å); [4] The offset distance between two aromatic rings (Å).

Table S6. π···π interactions in **1·dpt·1.5H$_2$O** at different temperatures.

80 K	θ[1]	Z[2]	d[3]	r[4]
py1[a] and py2[b]	11.676(244)	3.7225(2)	3.5601	1.0875
py2[b] and py3[c]	11.676(244)	3.5937(1)	3.2932	1.4386
py5[e] and py6[f]	5.515(229)	3.4269(1)	3.3456	0.7420
py7[g] and py8[h]	6.106(239)	3.7009(1)	3.6220	0.7601
py8[h] and py9[i]	6.106(239)	3.6915(1)	3.3629	1.5225
py11[k] and py12[l]	6.217(246)	3.6582(1)	3.6224	0.5105
180 K	θ[1]	Z[2]	d[3]	r[4]
py1[a] and py2[b]	12.754(291)	3.7570(2)	3.6314	0.9633
py2[b] and py3[c]	12.754(291)	3.6904(2)	3.3419	1.5655
py5[e] and py6[f]	5.262(251)	3.4869(2)	3.4279	0.6387
py7[g] and py8[h]	5.282(250)	3.7655(2)	3.6851	0.7740
py8[h] and py9[i]	5.282(250)	3.7260(2)	3.4267	1.4631
py11[k] and py12[l]	6.410(255)	3.7446(2)	3.6997	0.5781
298 K	θ[1]	Z[2]	d[3]	r[4]
py1[a] and py2[b]	10.907(362)	3.7759(4)	3.6542	0.9509
py2[b] and py3[c]	10.907(362)	3.7449(3)	3.5105	1.3041
py5[e] and py6[f]	6.220(323)	3.5966(3)	3.5401	0.6350
py7[g] and py8[h]	4.754(386)	3.8391(3)	3.7512	0.8168
py8[h] and py9[i]	4.754(386)	3.8616(3)	3.5483	1.5237
py11[k] and py12[l]	6.298(396)	3.8020(3)	3.7645	0.5327

[a]py1: C5-C9, N5, x, y, z; [b]py2: C60-C64, N16, 1-x, 1/2+y, 1/2-z; [c]py3: C5'-C9', N5', 1+x, y, z; [e]py5: C37-C41, N13, x, 3/2-y, 1/2+z; [f]py6: C14'-C18', N6', 1+x, y, z; [g]py7: C32-C36, N12, x, 3/2-y, 1/2+z; [h]py8: C51-C55, N15, 1-x, 1/2+y, 1/2-z; [i]py9: C32'-C36', N12', 1+x, 3/2-y, 1/2+z; [k]py11: C46-C50, N14, x, 3/2-y, 1/2+z; [l]py12: C23'-C27', N11', 1+x, 3/2-y, 1/2+z.

[1] The dihedral angle between two aromatic rings (°); [2] The distance between the centroids of aromatic rings (Å); [3] The perpendicular distance between two aromatic rings (Å); [4] The offset distance between two aromatic rings (Å).

Table S7. Hydrogen-bonding interactions in **1·dpt·2.5H$_2$O** at different temperatures.

T	I[1]			II[2]			III[3]		
	D-H···A	**d(D···A)**	**<(DHA)**	**D-H···A**	**d(D···A)**	**<(DHA)**	**D-H···A**	**d(D···A)**	**<(DHA)**
80 K				C8-H8…N13[a]	3.403	152.37	O1-H1B…N14	2.853	170.13
				C11-H11…N13[b]	3.587	165.67	O1-H1A…N15	2.857	171.19
150 K	C17-H17…N9[c]	3.146	111.95	C8-H8…N13	3.415	152.75	O1-H1B…N14	2.869	168.62
				C11-H11…N13	3.594	165.68	O1-H1A…N15	2.862	168.89
298 K				C8-H8…N13	3.445	156.73	O1-H1B…N14	2.985	165.81
							O1-H1A…N15	2.963	165.18

[1] Hydrogen-bonding interactions between host and host; [2] Hydrogen-bonding interactions between host and guests. [3] Hydrogen-bonding interactions between guests. Symmetry code: a) 1-x, -1/2+y, 1/2-z; b) 1-x, -1/2+y, 1/2-z; c) 1-x, 1-y, 1-z.

Table S8. Hydrogen-bonding interactions in **1·dpt·1.5H$_2$O** at different temperatures.

T	I[1]			II[2]			III[3]		
	D-H···A	**d(D···A)**	**<(DHA)**	**D-H···A**	**d(D···A)**	**<(DHA)**	**D-H···A**	**d(D···A)**	**<(DHA)**
80 K				C8-H8…N13[a]	3.395	152.13	O1-H1B…N14	2.957	173.29
				C11-H11…N13[b]	3.611	166.19	O1-H1A…N15	2.887	175.87
180 K	C17-H17…N9[c]	3.136	112.45	C8-H8…N13	3.426	152.54	O1-H1B…N14	2.929	173.11
							O1-H1A…N15	2.899	171.13
298 K	C7-H7…N7	3.208	114.20	C8-H8…N13	3.431	156.24	O1-H1B…N14	2.999	169.59
							O1-H1A…N15	2.930	168.00

[1] Hydrogen-bonding interactions between host and host; [2] Hydrogen-bonding interactions between host and guests. [3] Hydrogen-bonding interactions between guests. Symmetry code: a) 1-x, -1/2+y, 1/2-z; b) 1-x, -1/2+y, 1/2-z; c) 1-x, 1-y, 1-z.

(a)

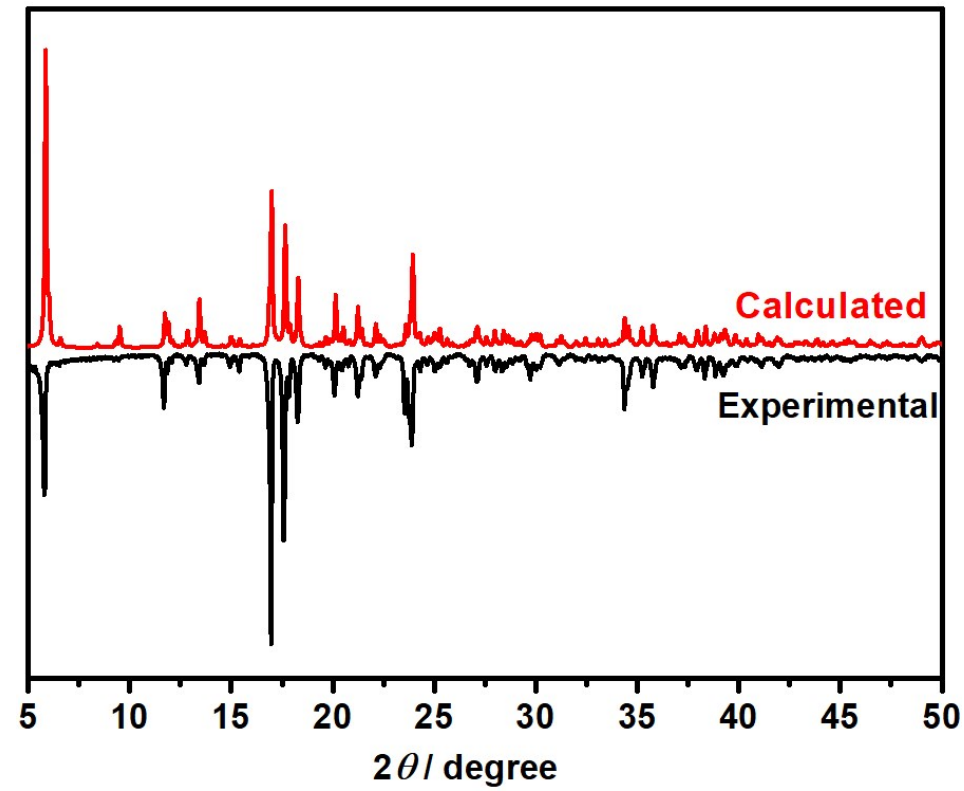
Calculated
Experimental
5
10
15
20
25
30
35
40
45
50
2θ / degree

(b)

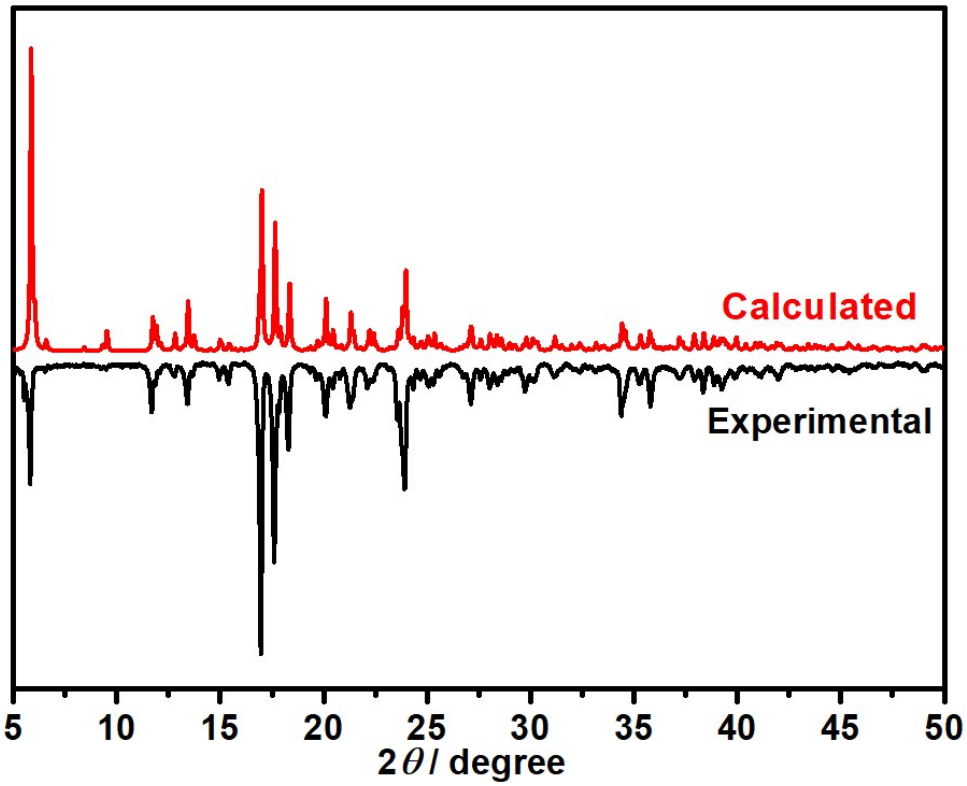
Calculated
Experimental
5
10
15
20
25
30
35
40
45
50
2θ / degree

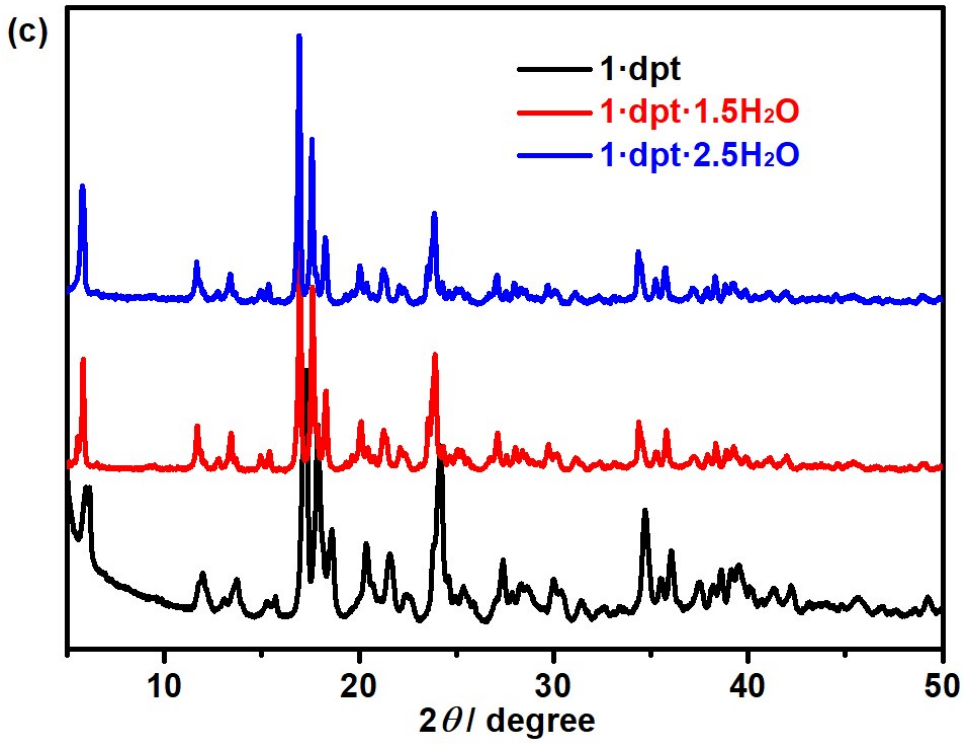

Figure S1. Powder X-ray diffraction data for **1·dpt·2.5H$_2$O** (a) and **1·dpt·1.5H$_2$O** (b) at room temperature. (c) The experimental PXRD patterns for **1·dpt·2.5H$_2$O, 1·dpt·1.5H$_2$O** and **1·dpt** at room temperature. The fully dehydrated phase **1·dpt** was obtained by heating the old samples of **1·dpt·1.5H$_2$O** (aged about half a year) at 107 °C for 2.5 h.

(a)

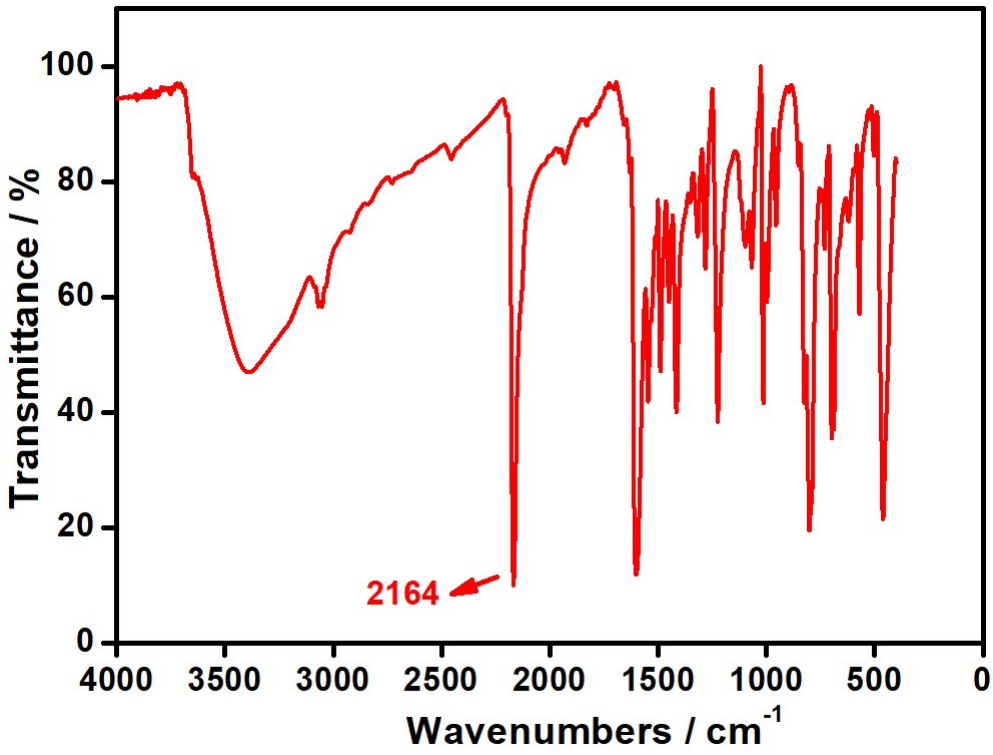
Transmittance / %
100
80
60
40
20
0
2164
4000
3500
3000
2500
2000
1500
1000
500
0
Wavenumbers / cm-1

(b)

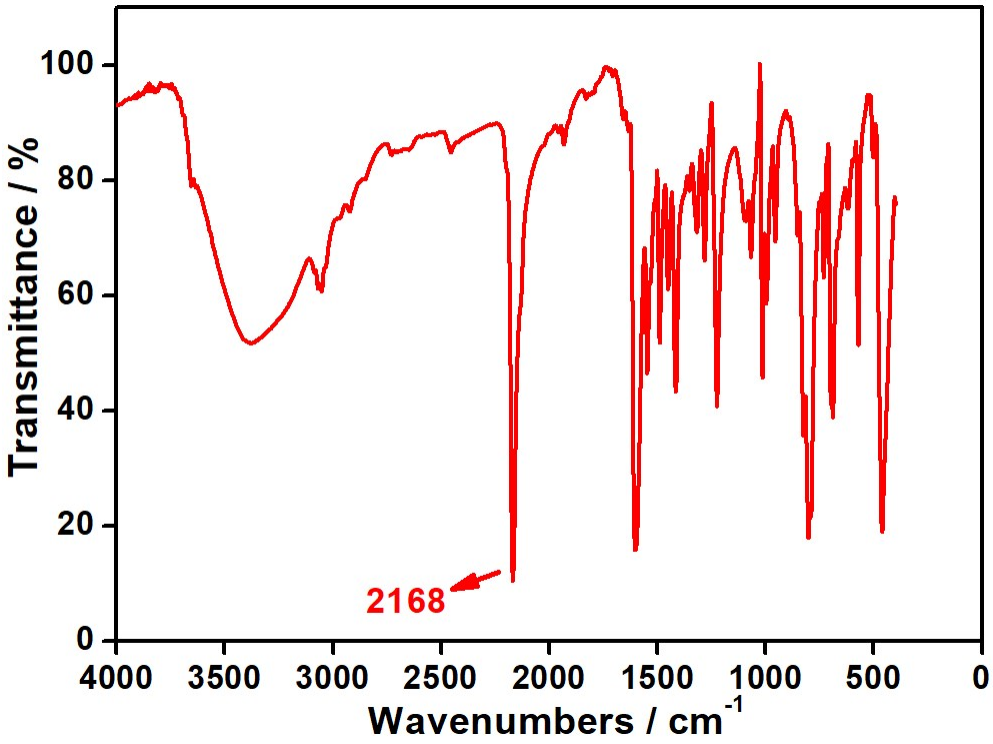
Transmittance / %
100
80
60
40
20
0
2168
4000
3500
3000
2500
2000
1500
1000
500
0
Wavenumbers / cm-1

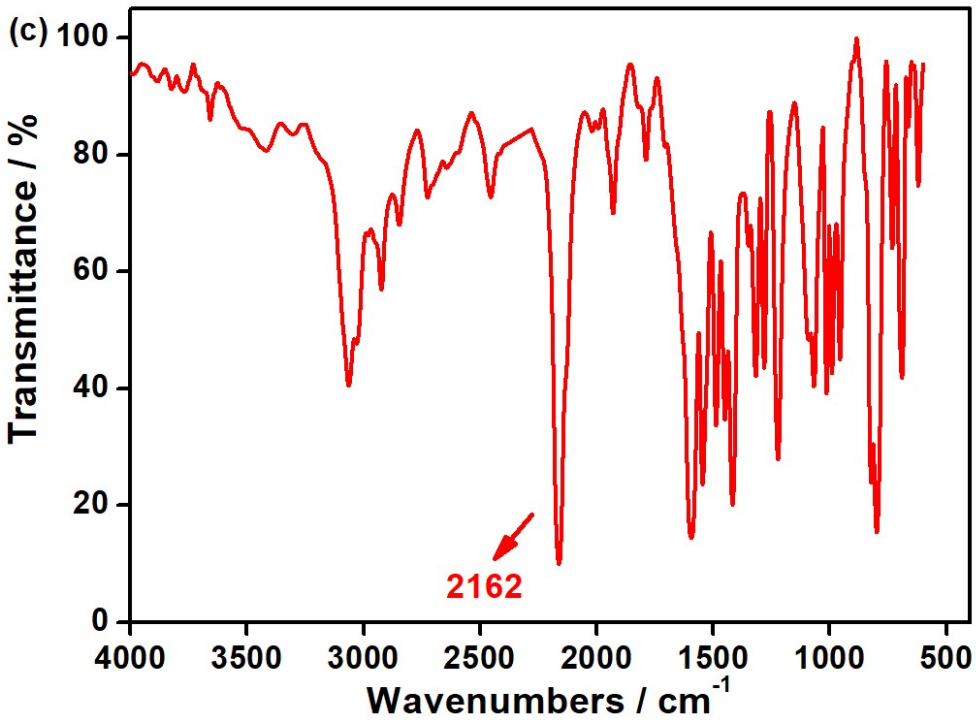

Figure S2. The FT-IR spectra of **1·dpt·2.5H$_2$O** (a), **1·dpt·1.5H$_2$O** (b) and **1·dpt** (c). The characteristic band at 2164 cm^{-1} in **1·dpt·2.5H$_2$O**, 2168 cm^{-1} in **1·dpt·1.5H$_2$O** and 2162 cm^{-1} in **1·dpt** are attributed to the stretching vibration of cyano group. **1·dpt** was obtained by heating the old samples of **1·dpt·1.5H$_2$O** (aged about half a year) at 107 °C on a BRUKER VERTEX70 FT-IR spectrometer.

(a)

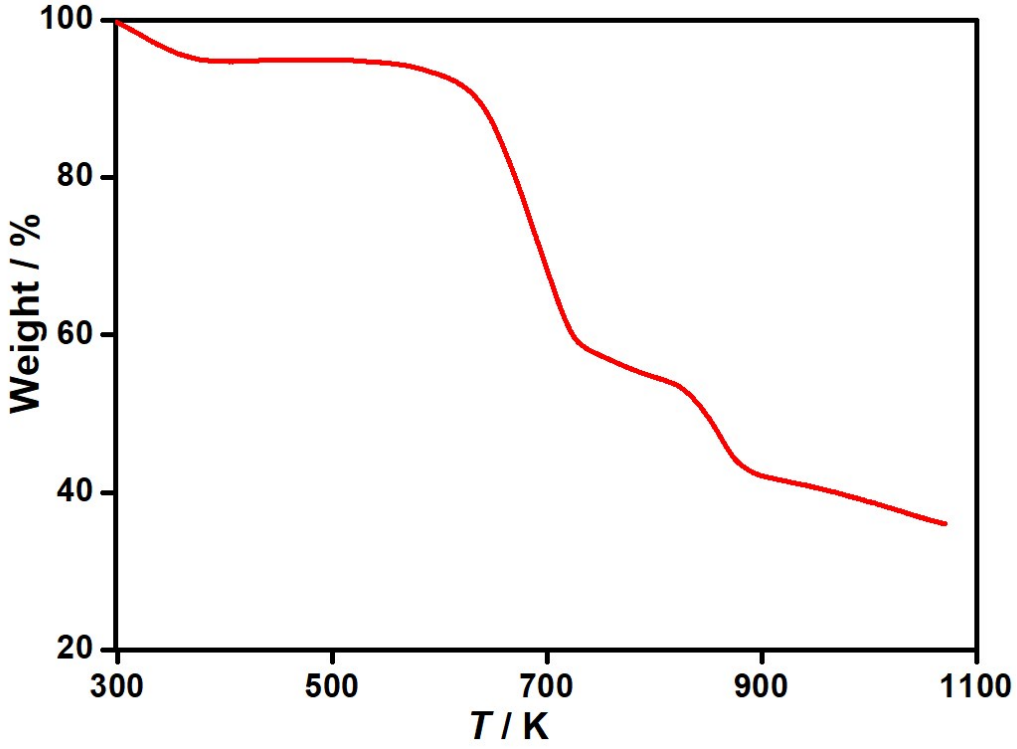
100
80
60
40
20
Weight / %
300
500
700
900
1100
T / K

(b)

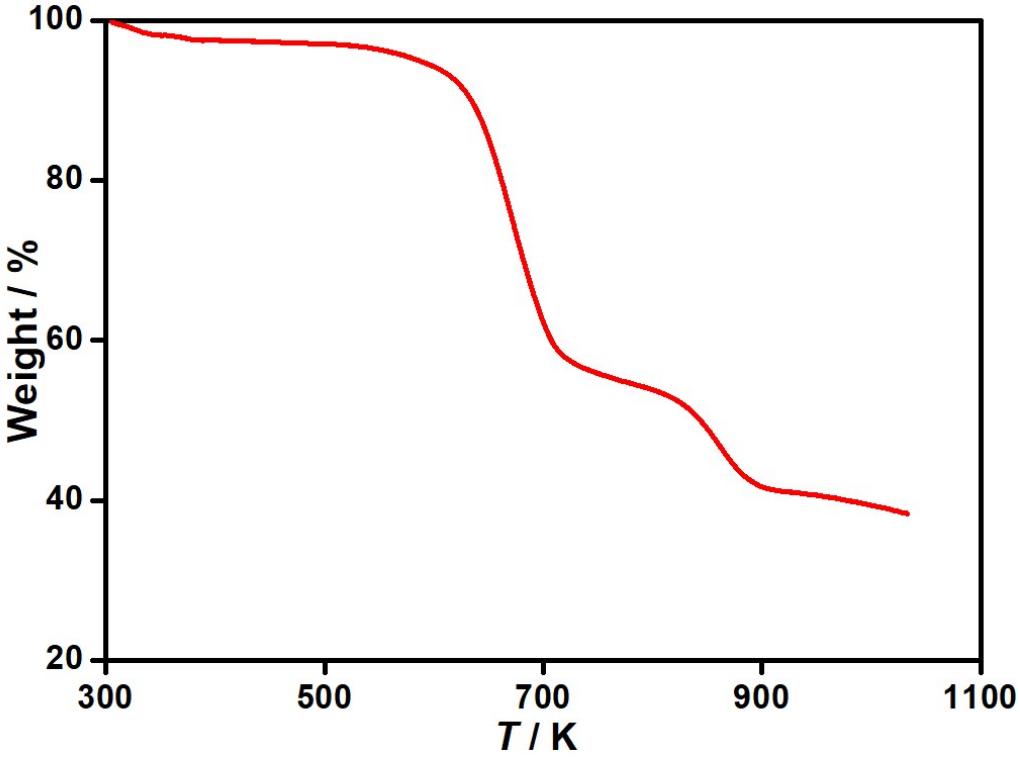
100
80
60
40
20
Weight / %
300
500
700
900
1100
T / K

(c)

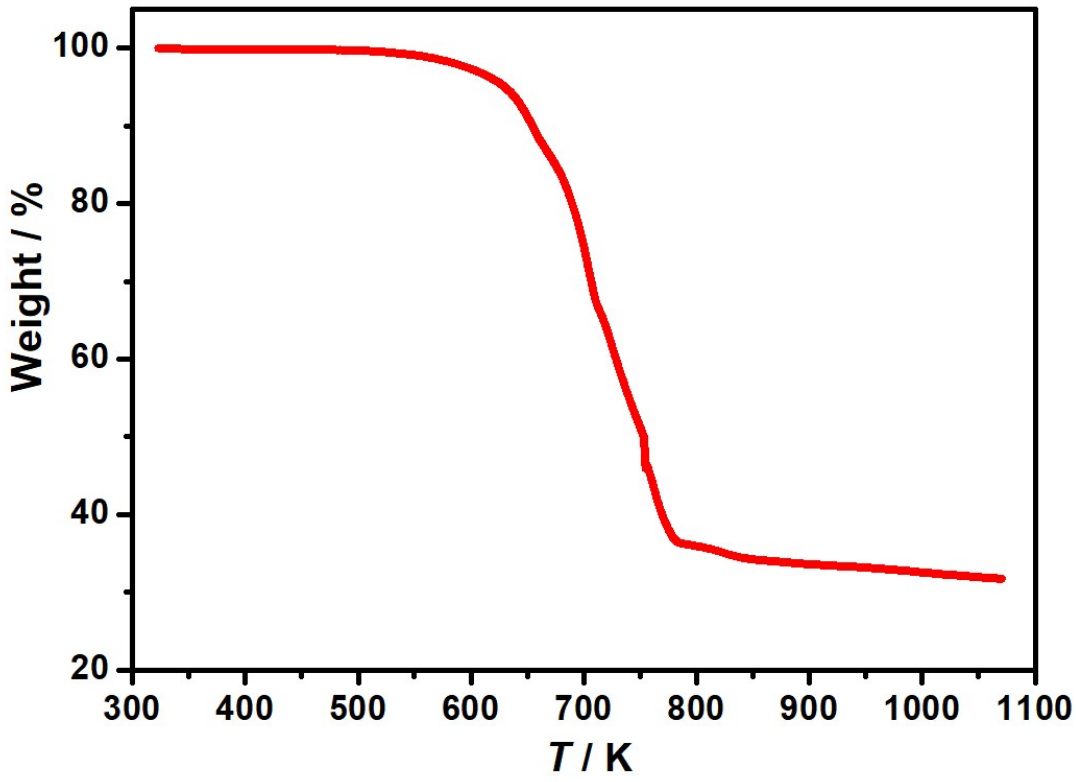

Figure S3. Thermogravimetric analyses of **1·dpt·2.5H$_2$O** (a), **1·dpt·1.5H$_2$O** (b) and **1·dpt** (c). The weight loss of **1·dpt·2.5H$_2$O** (5.04 %) and **1·dpt·1.5H$_2$O** (3.00 %) are close to the weight percent of 2.5 H_2O (5.13 %) and 1.5 H_2O (3.14 %). The fully dehydrated phase **1·dpt** was obtained by heating the old samples of **1·dpt·1.5H$_2$O** (aged about half a year) at 107 °C for 2.5 h.

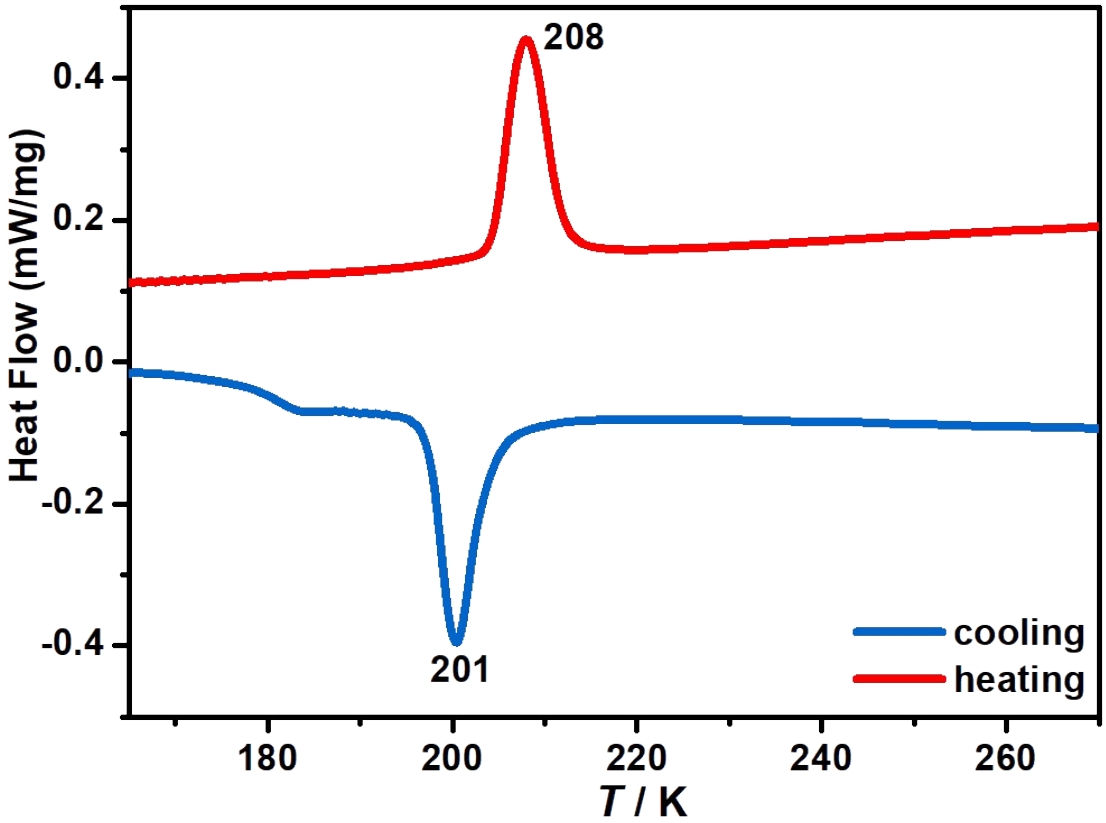

Figure S4. The differential scanning calorimetry (DSC) curves at 10 K min^{-1} for **1·dpt·1.5H$_2$O** in the cooling (blue) and warming (red) modes. The exothermic peak at 201 K and endothermic peak at 208 K in DSC curve are close to the T_c values for the first-step spin transition from the magnetic susceptibility data. However, the T_c values for the second-step spin transition are too low to be measured in the DSC instrument. As for the humid samples of **1·dpt·2.5H$_2$O**, the freezing point of mother liquor (equal volume of methanol and water) will affect the DSC curve, which can't be obtained accurately.

(a)

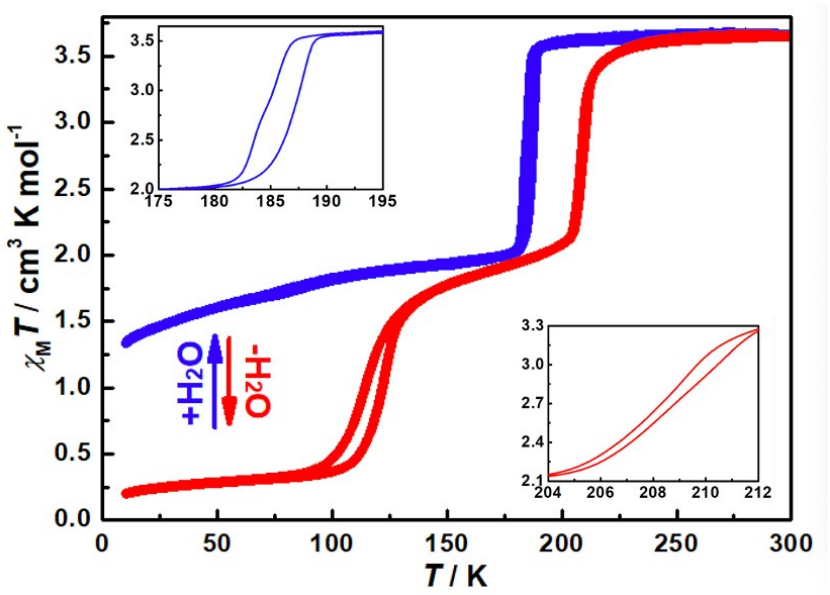

(b)

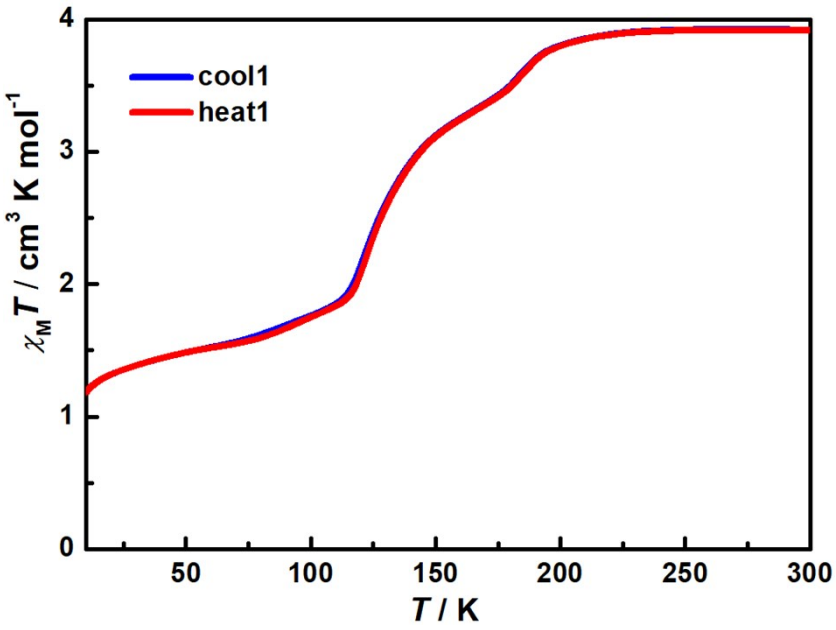

Figure S5. Temperature-dependence magnetic susceptibility data for **1·dpt·2.5H$_2$O** (blue) and **1·dpt·1.5H$_2$O** (red) at 2 K min^{-1} (a) and for **1·dpt** in settle mode (b). The inset graph illustrates the hysteresis loop for **1·dpt·2.5H$_2$O** (up) and **1·dpt·1.5H$_2$O** (down). **1·dpt** is generated by heating the old samples of **1·dpt·1.5H$_2$O** (aged about half a year) at 107 °C for 2.5 h on the SQUID magnetometer. The spin crossover behavior of **1·dpt** can be reproduced, although the $\chi_M T$ values at low temperatures for **1·dpt** generated from the aged samples of **1·dpt·1.5H$_2$O** are slightly higher than those for **1·dpt** generated from the fresh samples of **1·dpt·1.5H$_2$O**.

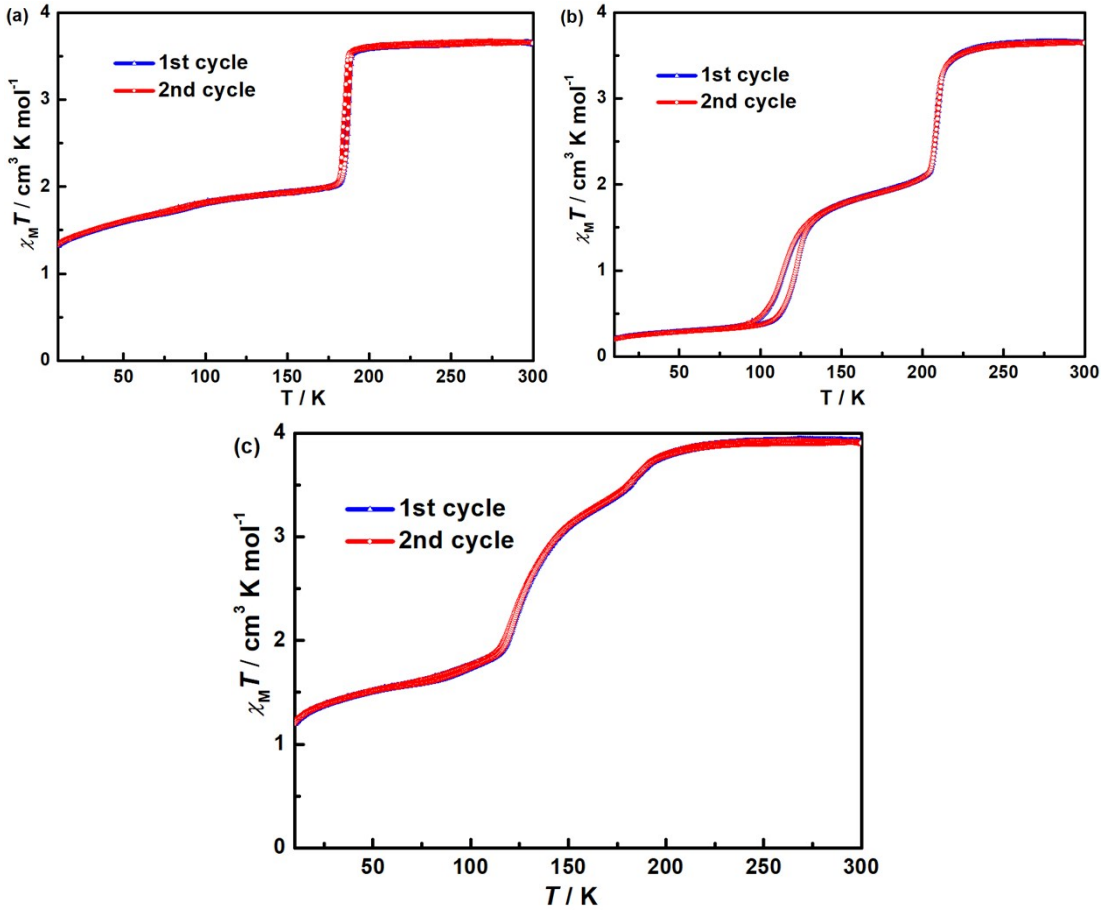

Figure S6. Variable-temperature magnetic susceptibility with two consecutive cycles for **1·dpt·2.5H$_2$O** (a), **1·dpt·1.5H$_2$O** (b) and **1·dpt** (c) at the scanning rate of 2 K min^{-1}. **1·dpt** is generated by heating the old samples of **1·dpt·1.5H$_2$O** (aged about half a year) at 107 °C for 2.5 h on the SQUID magnetometer.

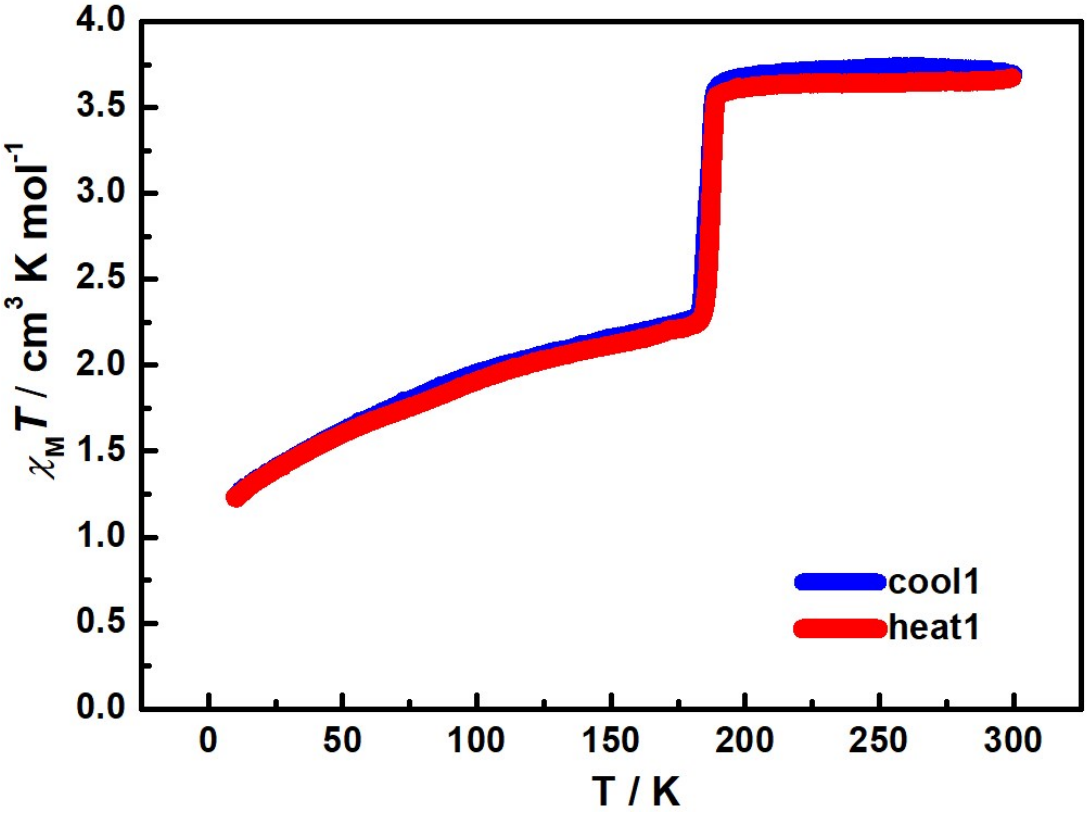

Figure S7. Temperature-dependence magnetic susceptibility data at 2 K min^{-1} for the water re-adsorption phase **1·dpt·2.5H$_2$O**, which is obtained by soaking **1·dpt·1.5H$_2$O** in water.

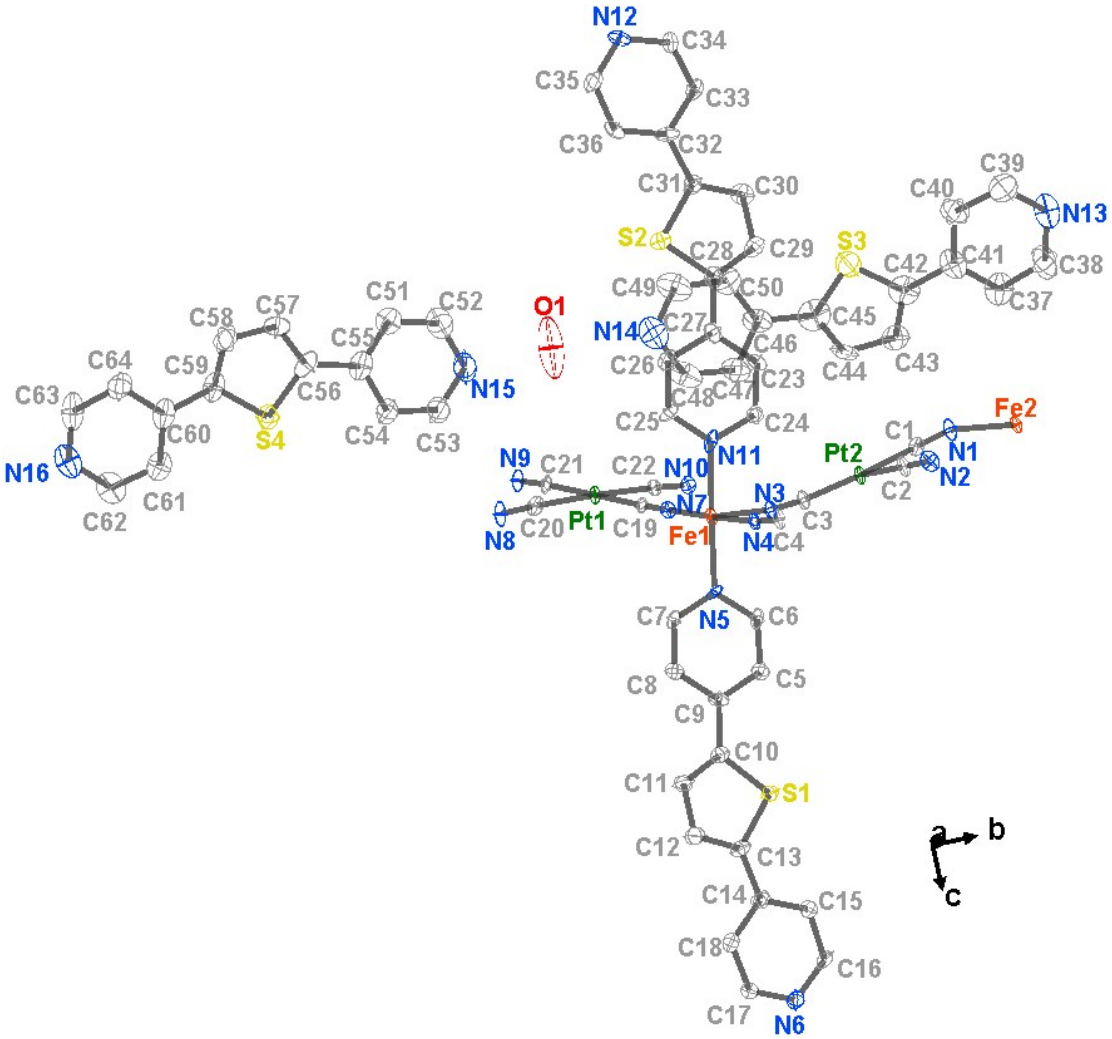

Figure S8. Asymmetric unit of **1·dpt·2.5H$_2$O** at 150 K. Thermal ellipsoids are drawn at the 30 % probability. Hydrogen atoms are omitted for clarity.

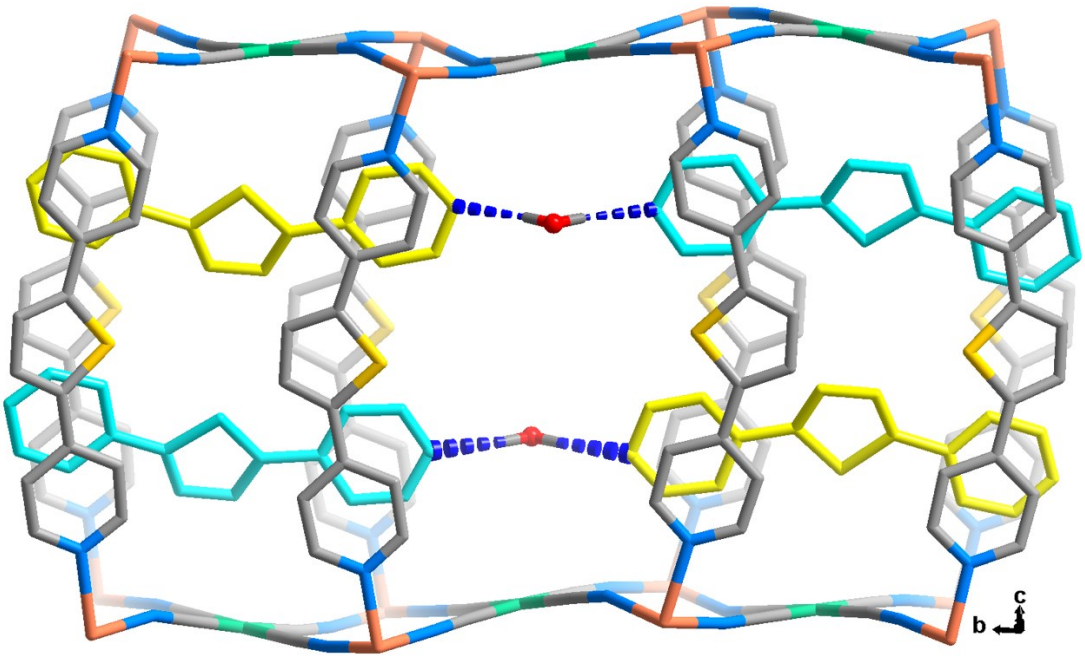

Figure S9. Structure representations along the *a*-axis for **1·dpt·2.5H$_2$O** at 150 K. The hydrogen-bonding interactions between water and the uncoordinated dpt ligands (dpt3, turquoise; dpt4, yellow) are shown as the blue dashed lines. Hydrogen atoms expect water are omitted for clarity. Color codes: Fe, orange; Pt, green; N, blue; C, grey; S, yellow; O, red.

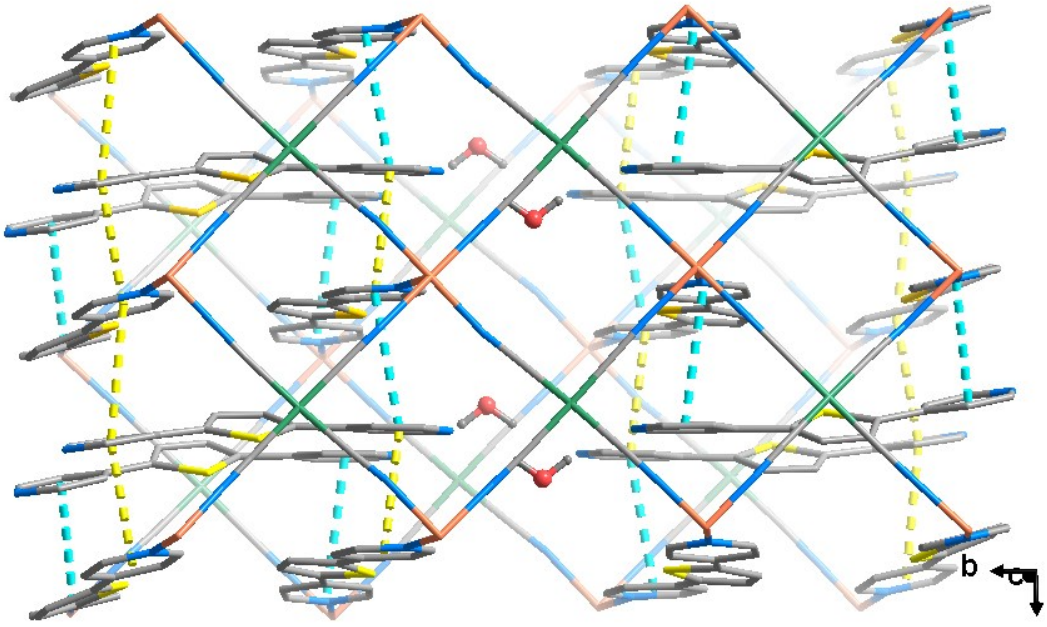

Figure S10. Offset face-to-face (yellow dashed lines) and face-to-face π···π interactions (turquoise dashed lines) in **1·dpt·2.5H$_2$O** at 150 K along the *c* axis.

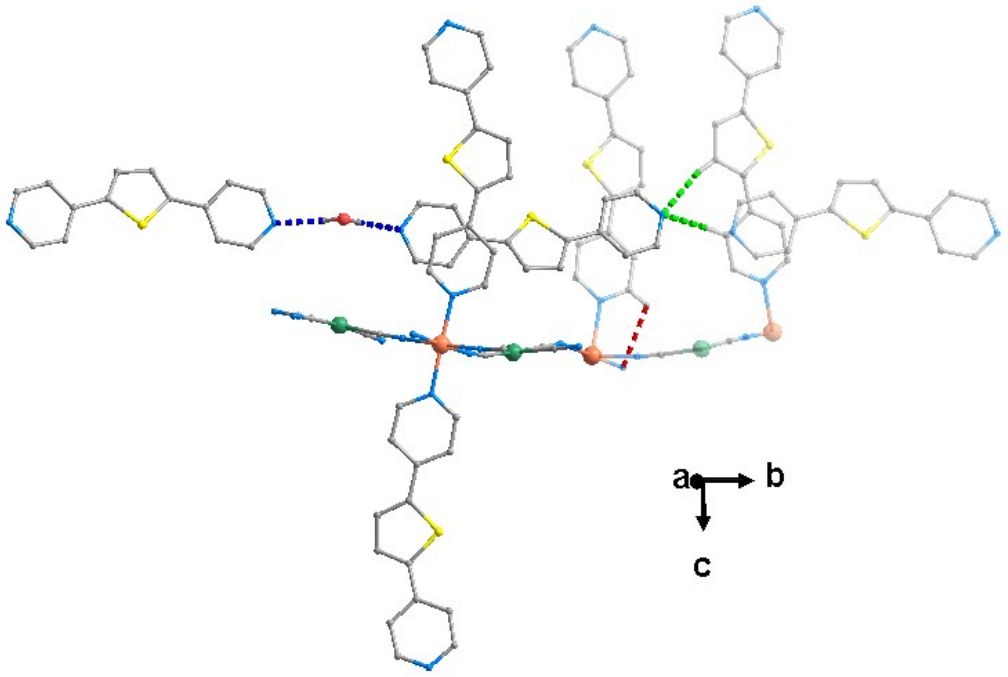

Figure S11. The bifurcated H-bonds (C8−H8···N13···H11−C11, green dashed lines), the strong H-bonds (O1−H···N14 and O1−H···N15, blue dashed lines) and the H-bonds of C17-H17···N9 (red dashed lines) in **1·dpt·2.5H_2O** at 150 K. The molecules in the asymmetric unit are highlighted while the molecules generated by the symmetry codes are translucent. Only the hydrogen atoms involving the hydrogen-bonding interactions are shown while and the others are omitted for clarity. Color codes: Fe, orange; Pt, green; O, red; C, grey; N, blue; H, dark grey.

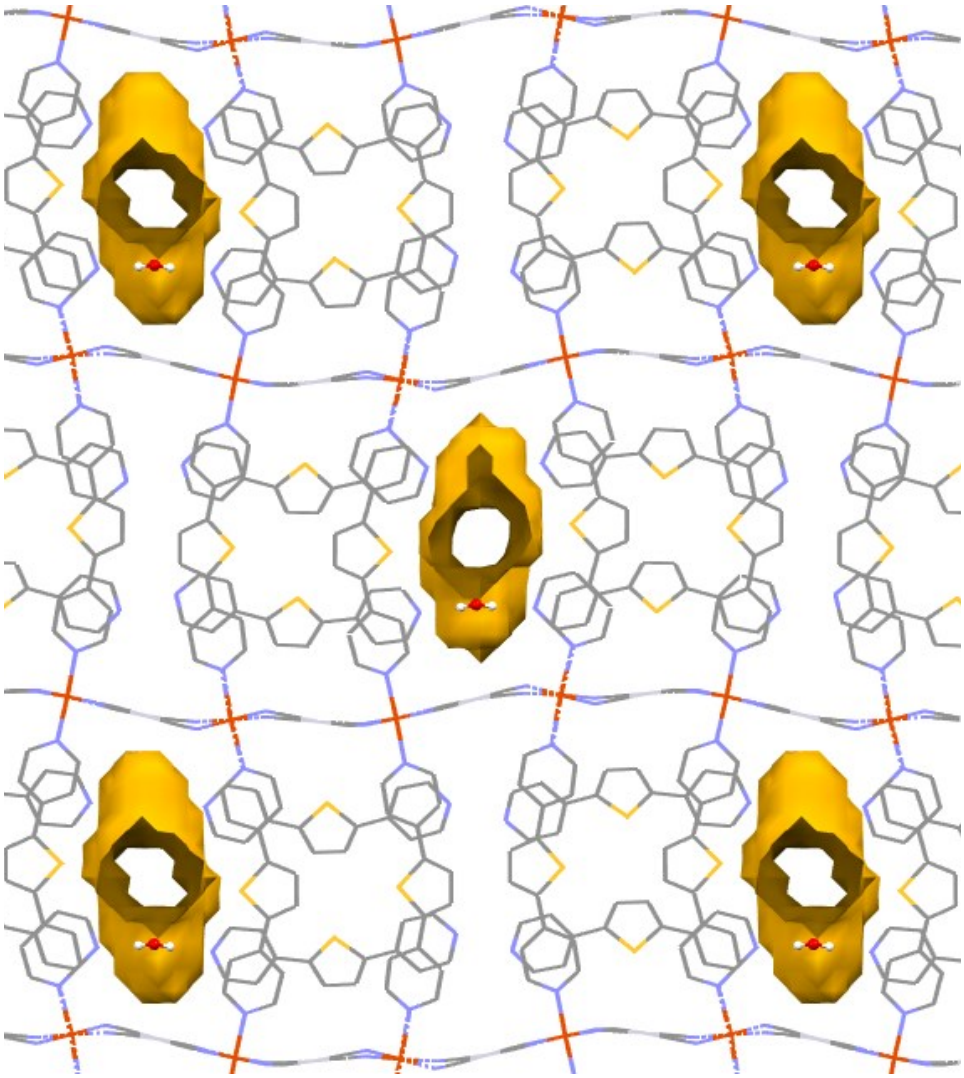

Figure S12. The voids along the *a*-axis in the framework of **1·dpt·2.5H$_2$O** at 150 K.

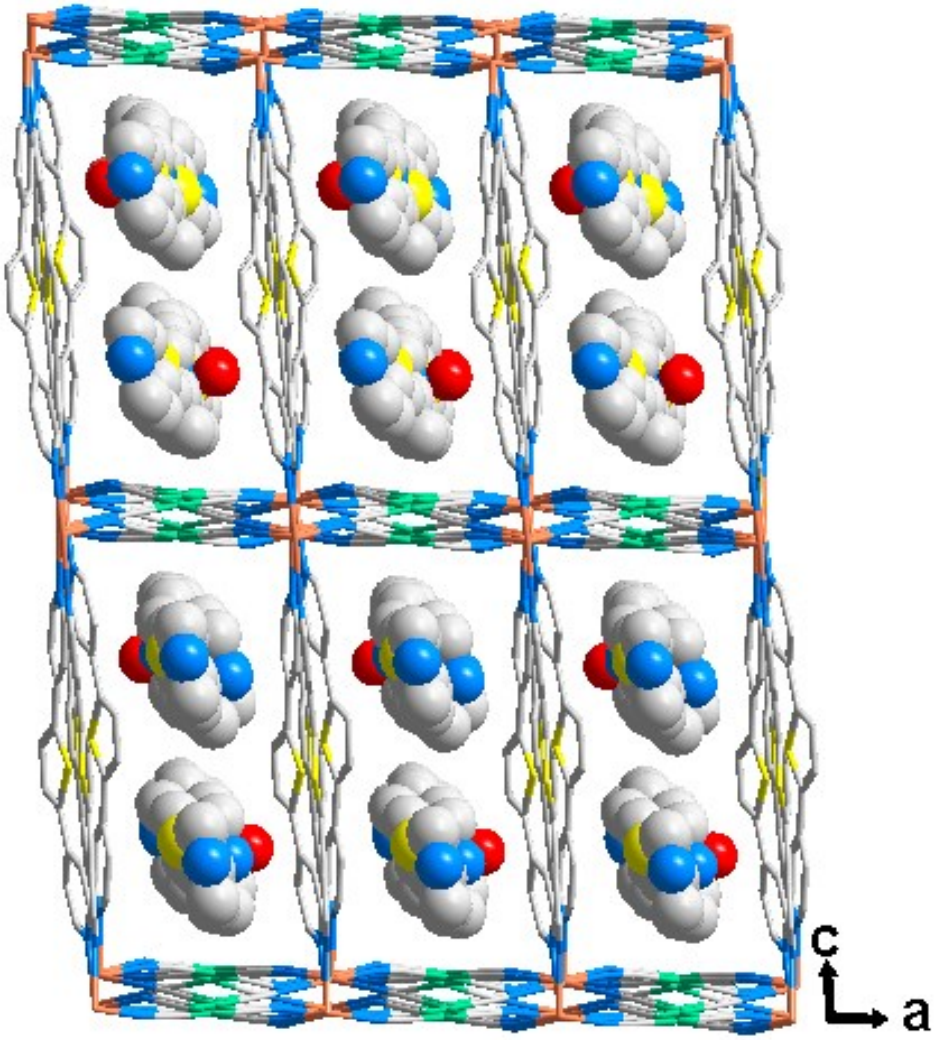

Figure S13. The uncoordinated dpt ligands (space-filling) and H_2O in the 1D channels along the *b*-axis within the 3D framework of **1·dpt·2.5H$_2$O** at 150 K. Hydrogen atoms are omitted for clarity.

(a)

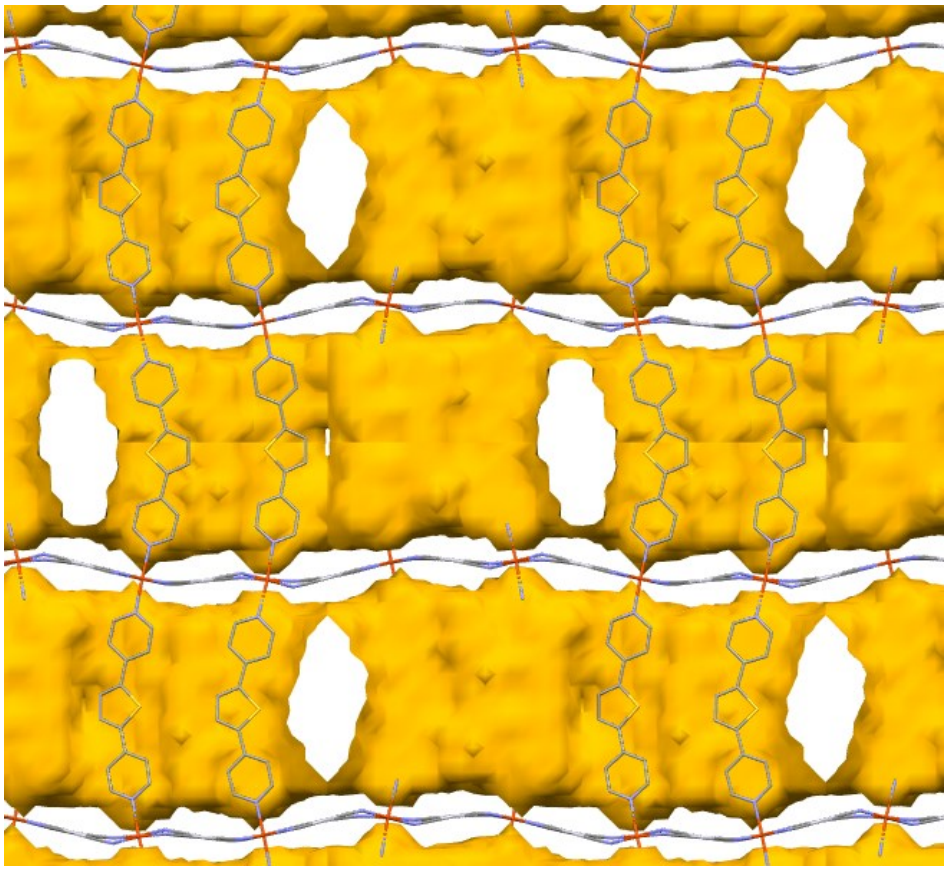

(b)

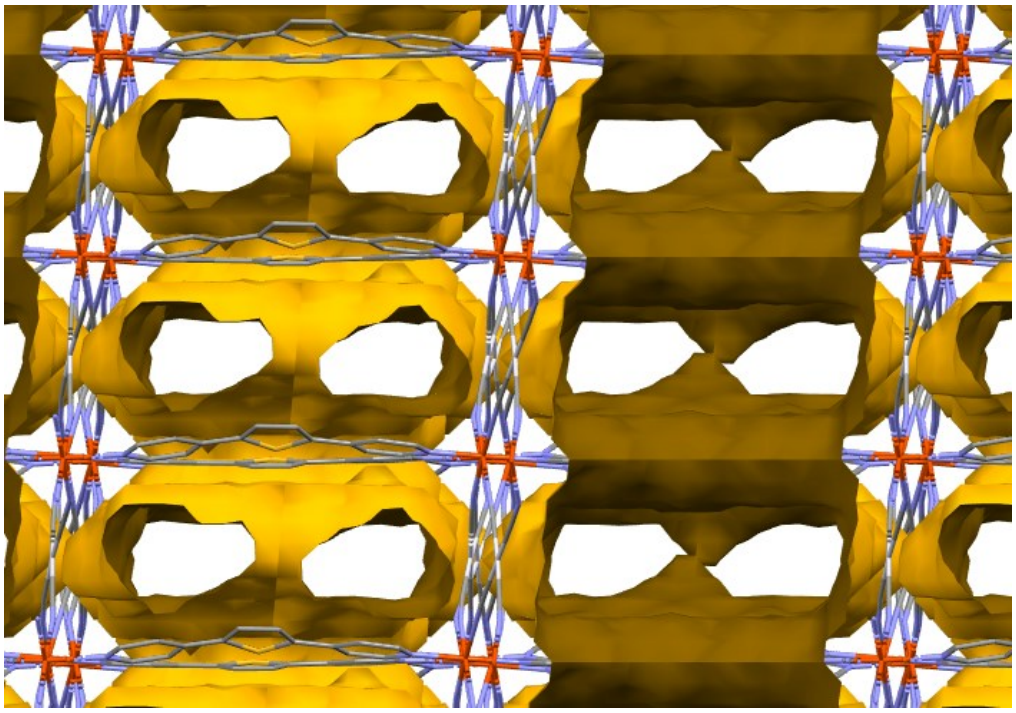

Figure S14. 1D channels along the *a*-axis (a) and the *b*-axis (b) for **1·dpt·2.5H$_2$O** at 150 K after removing the uncoordinated dpt ligands and H_2O.

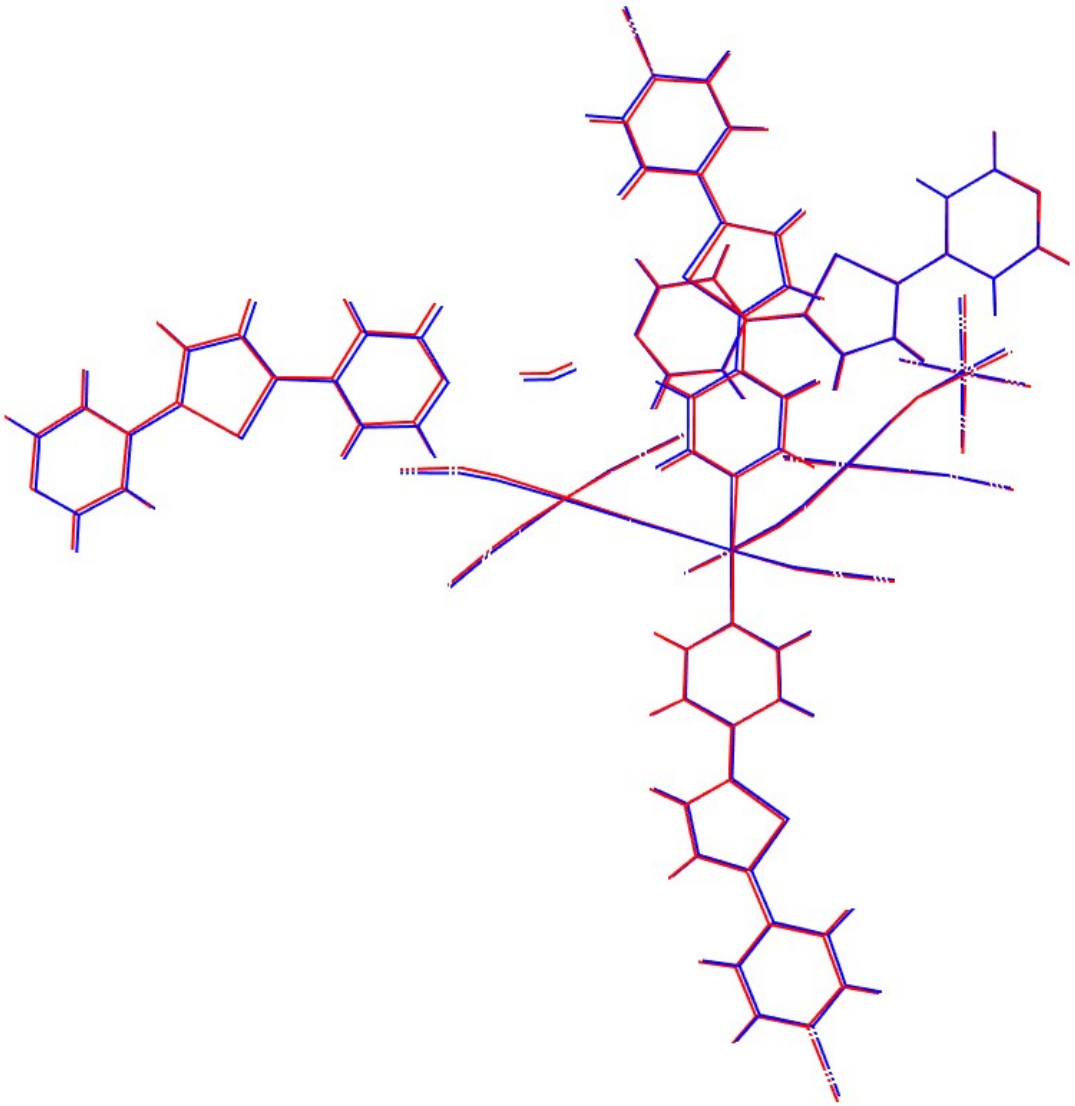

Figure S15. The structural overlap for the asymmetric units of **1·dpt·2.5H$_2$O** (red) and **1·dpt·1.5H$_2$O** (blue) at 80 K.